



HAL
open science

Ultrasound characterization of aggregated red blood cells: towards in vivo application

Emilie Franceschini, François T. H. Yu, Guy Cloutier

► **To cite this version:**

Emilie Franceschini, François T. H. Yu, Guy Cloutier. Ultrasound characterization of aggregated red blood cells: towards in vivo application. Research Network GDR 2501, Jun 2008, France. pp.293-302. hal-00443787

HAL Id: hal-00443787

<https://hal.science/hal-00443787>

Submitted on 4 Jan 2010

HAL is a multi-disciplinary open access archive for the deposit and dissemination of scientific research documents, whether they are published or not. The documents may come from teaching and research institutions in France or abroad, or from public or private research centers.

L'archive ouverte pluridisciplinaire **HAL**, est destinée au dépôt et à la diffusion de documents scientifiques de niveau recherche, publiés ou non, émanant des établissements d'enseignement et de recherche français ou étrangers, des laboratoires publics ou privés.

Ultrasound characterization of aggregated red blood cells: towards *in vivo* application

Emilie Franceschini, François T. H. Yu, Guy Cloutier

Laboratory of Biorheology and Medical Ultrasonics

University of Montreal Hospital Research Center

2099 Alexandre de Sève (room Y-1619),

Montréal, Québec, H2L 2W5, Canada

franceschini@lma.cnrs-mrs.fr

Abstract

Ultrasonic backscattered signals from blood contain frequency-dependent information that can be used to obtain quantitative parameters reflecting the aggregation state of red blood cells (RBCs). The difficulty to use this frequency-dependent information *in vivo* is due to the attenuation caused by intervening tissue layers that distorts the spectral content of backscattering properties from blood microstructures. We propose an optimization method to simultaneously estimate tissue attenuation and blood structure factor. In an *in vitro* experiment, we obtained satisfactory estimates with relative errors below 25% for attenuations between 0.115 and 0.411 dB/cm/MHz and $D < 10$ (D the aggregate diameter expressed in number of RBCs).

1. Introduction

For the detection and characterization of tissues, quantitative ultrasound techniques using the radio frequency (rf) backscattered signals have received broad interest for the past 30 years. One approach is to use the magnitude and the frequency dependence of the rf backscatter spectrum in order to quantify the tissue structures such as the size, acoustic impedance, and concentration of the scatterers. Many *in vitro* and *in vivo* experiments have been performed to demonstrate the utility of this approach for characterizing of eye, liver, kidney, prostate and breast. Recently, the frequency dependence of the ultrasound backscattering coefficient (BSC) was studied to assess the level of red blood cell (RBC) aggregation. Two parameters describing RBC aggregation, the packing factor and mean aggregate diameter, were estimated from the Structure Factor Size Estimator (SFSE).¹ The difficulty to use the SFSE *in vivo* is that the spectral content of backscattered signals is also affected by attenuation caused by intervening tissue layers between the probe and the blood flow. More generally, ultrasound scatterer size estimation techniques for tissue characterization (such as liver, kidney, prostate or breast) has had limited success in clinical practice because of tissue attenuation effects.^{2,3} Some groups^{2,4,5} developed measurement methods to evaluate the frequency-dependent attenuation in order to compensate *a posteriori* the backscattered power spectrum. Our goal is to explore an other strategy for *in vivo* measures of RBC scatterer sizes. Recently, we propose an optimization method providing an estimate of total attenuation and blood structural parameters simultaneously, termed the Structure Factor Size and Attenuation Estimator (SFSAE).⁶ This method consists in fitting the spectrum of the backscattered radio-frequency (rf) echoes from blood to an estimated spectrum by a modified SFSE model. Herein, the SFSAE is improved and *in vitro* experimental evaluation of the SFSAE is performed.

2. Background: Structure Factor Size and Attenuation Estimator

The technique allowing to estimate simultaneously blood structural parameters and total attenuation has been described in detail in Ref. 6 and is summarized here.

Blood can be considered as a very dense suspension of particles (i.e. red cells) having strong interactions (collision, attraction, deformation, flow dependent motions). We develop a theoretical model of blood ultrasound backscattering based on the particle approach.^{7,8} This approach consists of summing contributions from individual RBCs and models the RBC interaction by a particle pair-correlation function. The model proposed in Ref. 1 has been modified to predict the theoretical backscatter coefficient from blood:⁶

$$BSC_{theor}(k) = m\sigma_b(k)S(k)A(k) \quad (1)$$

where k is the wave vector, m is the number density of RBCs in blood estimated by measuring the hematocrit H by microcentrifugation ($m = H/V_s$, where V_s is the volume of a RBC), σ_b is the backscattering cross section of a single RBC, S is the structure factor describing the spatial organization of RBCs, and A is the frequency-dependent attenuation function. The backscattering cross-section σ_b of a weak scattering particle small compared to the wavelength (Rayleigh scatterer) can be determined analytically as follows: $\sigma_b(k) = 1/(4\pi^2)k^4V_s^2\gamma_z^2$, where γ_z is the variation of impedance between the RBC and its suspending medium (i.e. the plasma). The structure factor S is the Fourier transform of the pair-correlation function⁸ g and is approximated by its second-order Taylor expansion¹ in k as

$$S(k) = 1 + m \int (g(r) - 1) e^{-2jkr} dr \approx W - \frac{12}{5}(kR)^2. \quad (2)$$

In this last equation, W is the low-frequency limit of the structure factor ($S(k)|_{k \rightarrow 0}$) called the packing factor.^{8,9} R is the radius of 3D RBC aggregates assumed to be isotropic. We introduce $D = R/a$ as the isotropic diameter of an aggregate (expressed in number of RBCs) with a the radius of one RBC sphere-shaped model of volume V_s . The attenuation function A is given by: $A(k) = e^{-4\alpha_0 f}$, where f is the frequency and α_0 is the attenuation coefficient (in dB/MHz) defined by: $\alpha_0 = \sum_i \alpha_i e_i$, where α_i and e_i are respectively the intervening tissue layer attenuations (in dB/cm/MHz) and thicknesses. We thus assume that the attenuation increases linearly with the frequency: $\alpha(f) = \alpha_0 f$.

The measured backscatter coefficient was computed as

$$BSC_{meas}(k) = BSC_{ref}(k) \frac{\overline{P_{meas}(k)}}{\overline{P_{ref}(k)}}. \quad (3)$$

In Eq. (3), the mean backscattered power spectrum $\overline{P_{meas}}$ was obtained by averaging the power spectra of 20 backscattered echoes from blood. The mean power spectrum $\overline{P_{ref}}$ was obtained from a reference sample of non-aggregated RBCs at a low hematocrit of 6% (i.e. Rayleigh scatterers).¹⁰ In this case, 20 echoes were also averaged. This reference sample was used to compensate the backscattered power spectrum $\overline{P_{meas}}$ for the electromechanical system response, and the depth-dependent diffraction and focusing effects caused by the US beam.

The packing factor W , aggregate diameter D and total attenuation along the propagation path α_0 were determined by matching the measured BSC_{meas} given by Eq. (3) with the theoretical BSC_{theor} given by Eq. (1). For this purpose, we searched values of W , D and α_0 minimizing the cost function $F(W, D, \alpha_0) = ||BSC_{meas} - BSC_{theor}||^2$. In all studied cases, the cost function seemed to have a unique global minimum, as was observed by plotting the cost function surface $F(W, D)$ with varying values of α_0 (see Fig. 1 in Ref. 6). For the optimization problem, we defined a set of lower and upper bounds on the variables (W , D , α_0) so that the solution is searched in the range: $0 \leq W \leq 100$, $0 \leq D \leq 50$ and $0 \leq \alpha_0 \leq 1$ dB/MHz. We chose to reject the solution (W , D , α_0) having an estimated diameter D very small compared to 0.1.

3. *In vitro* experiment in a Couette flow device

3.1 Blood preparation

Fresh porcine whole blood was obtained from a local slaughter house, centrifuged and the plasma and buffy coat were removed. Two blood samples were then prepared: (i) a H6 reference sample, which was a 6% hematocrit non-aggregating RBCs resuspended in saline solution; and (ii) a 40% hematocrit T40 test sample, which consisted of RBCs resuspended in plasma to promote aggregation.

3.2 Experimental set up

US measurements were performed in a Couette flow system to produce a linear blood velocity gradient at a given shear rate. The schematic configuration of the experience is shown in figure 1. The system consisted of a rotating inner cylinder with a diameter of 160 mm surrounded by a fixed concentric cylinder of diameter 164 mm. A 60 mL blood sample was sheared in the 2 mm annular space between the two coaxial cylinders. The US scanner (Vevo 770, Visualsonics, Toronto, Canada) equipped with the RMV 710 probe was used in B-mode. The single-element focused circular transducer had a center frequency of 25 MHz, a diameter of 7.1 mm and a focal depth of 15 mm. We operated at a sampling frequency of 250 MHz with 8 bits resolution (Gagescope, model 8500CS, Montreal, Canada). The probe was mounted in the side wall of the fixed outer cylinder and was positioned to have its focal zone at the center of both cylinders. To ensure ultrasonic coupling, the hole within the outer stationary cylinder (containing the probe) was filled with a liquid agar gel based mixture. When solidified, this gel was cut to match the curvature of the cylinder to avoid any flow disturbance. The gel was a mixture of distilled water, 3% (w/w) agar powder (A9799, Sigma Chemical, Saint-Louis, MO), 8% (w/w) glycerol and a specific concentration of 50 μm cellulose scattering particles (S5504 Sigmacell, Sigma Chemical, Saint-Louis, MO) that determined the attenuation coefficient. Five experiments were performed with five mixtures having Sigmacell (SC) concentrations varying from 0% to 1% (w/w). Since skin is one of the most attenuating tissue layers during *in vivo* scanning, phantoms were prepared in order to have attenuations closed from skin attenuation. The 0% concentration constituted the non-attenuating gel and the four other mixtures mimicked skin attenuations.

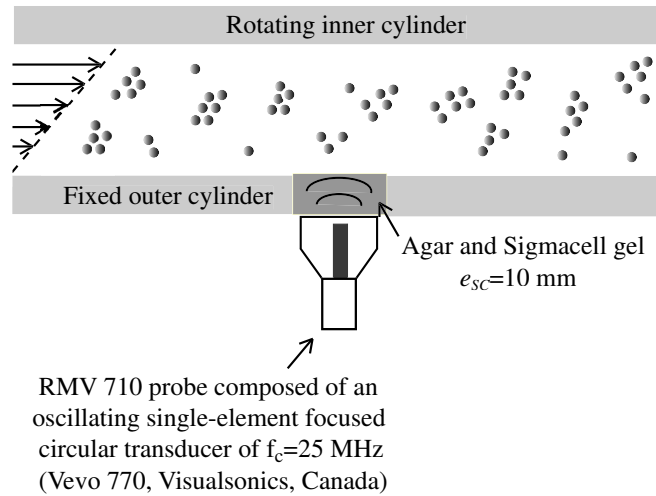


Figure 1: The Couette flow system

3.3 Attenuation measurements

The attenuation coefficients of the reference (0% SC) and of the others skin-mimicking phantoms α_{sc} were determined by using a standard substitution method. A transducer with center frequency of 25 MHz (Vevo 770, Visualsonics, Toronto, Canada) was used in transmission/reception with a reflector on the opposite side of the phantom for reflection measurements. Reflected signals were recorded both with and without the agar gel sample in the acoustic path. The attenuation coefficient was then estimated using a log spectral difference technique. For each concentration of SC, six regions were scanned for averaging purpose. Thicknesses of skin-mimicking phantoms e_{sc} were fixed to 10 mm. As shown in the table 1 summarizing results, attenuation coefficients of skin-mimicking phantoms were in the same range as the human dermis (0.21 dB/MHz at 14 - 50 MHz considering a 1 mm dermis thickness¹¹).

Attenuations of the blood α_{blood} sheared at different shear rates were also measured in the reflection mode using the same experimental configuration shown in figure 1. The gel had a 0% SC concentration and the rotating inner cylinder was used as the reflector. Table 2 summarizes results.

Table 1: Estimated values of the attenuation coefficients of the reference (0% SC) and of the others skin-mimicking phantoms (using a log spectral difference technique)

SC (%)	Sigmacell attenuation α_{sc} (dB/MHz)
0.25	0.115
0.5	0.219
0.75	0.320
1	0.412

Table 2: Estimated values of the blood attenuation sheared at different shear rates in the Couette flow device (using a log spectral difference technique)

Shear rates (s^{-1})	Blood attenuation α_{blood} (dB/MHz)
5	0.053
10	0.036
20	0.024
30	0.016
50	0.013

3.4 Measurement protocol

Prior to each measurement, the T40 blood was sheared at $200 s^{-1}$ during 30 s to disrupt RBC aggregates. The shear rate was then reduced to residual values of 5, 10, 20, 30 and $50 s^{-1}$ during 90 s to reach an equilibrium in the state of aggregation in the sheared blood sample. After that, for each shear rate, 20 B-mode images were constructed for 80 s. For each line of the B-mode images, echoes were selected with a rectangular window of length 0.4 mm at twenty depths every 0.04 mm (i.e. with 90% overlap between windows). For each depth, the power spectra of the backscattered echoes were averaged over 20 acquisitions (corresponding to the 20 acquired images) to provide P_{meas} . This protocol was repeated five times with the five agar-based phantoms. Then, the T40 blood was removed and the H6 sample was introduced in the Couette device. The H6 sample was sheared at $50 s^{-1}$ and coupled with the 0% SC concentration agar gel. Echoes were windowed as for the H40 sample at the same depths and their power spectra were averaged over 20 acquisitions to obtain P_{ref} .

3.5 Reference measurements with the 0% SC concentration phantom

The experiment with the 0% SC phantom was realized in order to have reference results on packing factors W_{ref} and aggregate diameters D_{ref} obtained from the classical SFSE.¹ These parameters were assumed to be true values of packing factors and aggregate diameters for all shear rates, and will be compared in the next section with packing factors and diameters estimated by the SFSAE and by the SFSE when skin-mimicking phantoms are used.

It is important to emphasize the fact that the H6 reference sample was also measured with the 0% SC phantom. The phantom attenuation, although small with no SC, therefore affected equivalently both spectra $\overline{P_{meas}}$ and $\overline{P_{ref}}$ in Eq. (3). The resulting measured backscatter coefficient BSC_{ref} was thus not biased by attenuation.

4. Results

4.1 Reference parameters with the SFSE

Figure 2 reports results on W_{ref} and D_{ref} from the SFSE with compensation for blood attenuation in the case of no gel attenuation. It can be observed that the amplitude of the backscattering coefficient as well as the estimation of the parameters on W_{ref} and D_{ref} decrease when the shear rate increases (i.e. the level of aggregation becomes smaller).

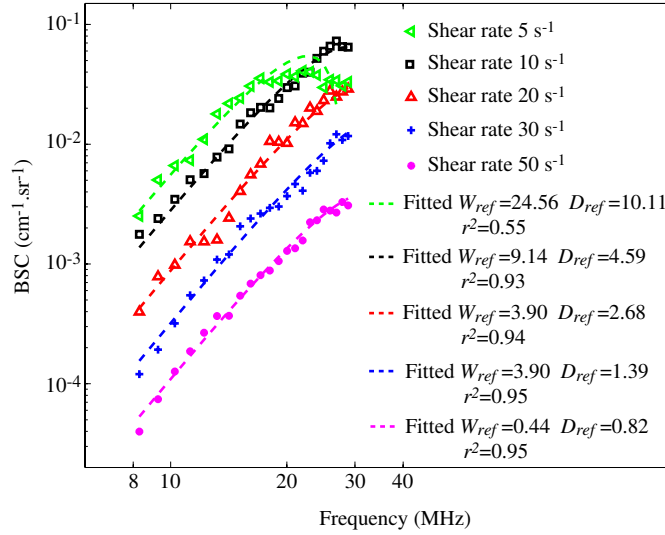


Figure 2: Backscatter coefficients for blood sheared at different residual shear rates and measured with the 0% SC concentration phantom, and corresponding fitting with the classical SFSE with no compensation for attenuation.

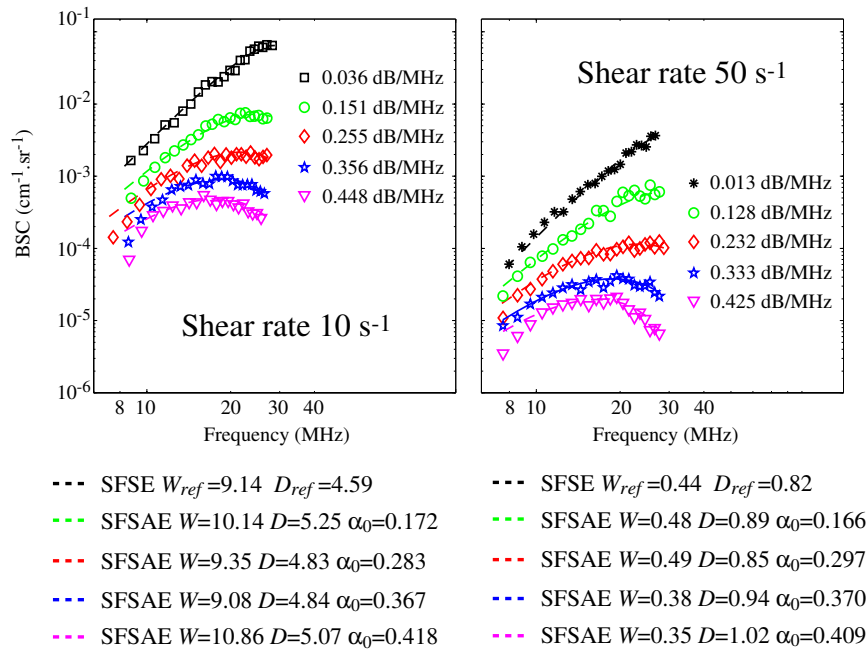


Figure 3: Backscatter coefficients for blood sheared at 10 s^{-1} and 50 s^{-1} , and measured with each of the five phantoms. The corresponding fitted models are the SFSE for the 0% SC phantom, and the SFSAE for the four other skin-mimicking phantoms (0.25, 0.5, 0.75 and 1% SC).

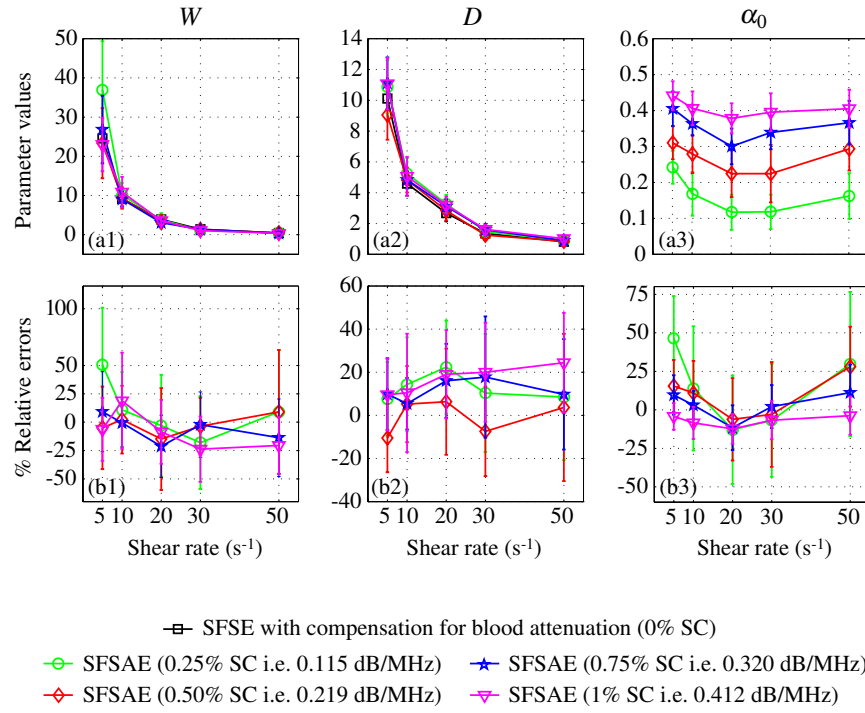


Figure 4: (a) Values of W , D and α_0 (in dB/MHz) for different residual shear rates estimated by the classical SFSE for the 0% SC concentration and by the SFSAE for the four skin-mimicking phantoms. (b) Corresponding relative errors.

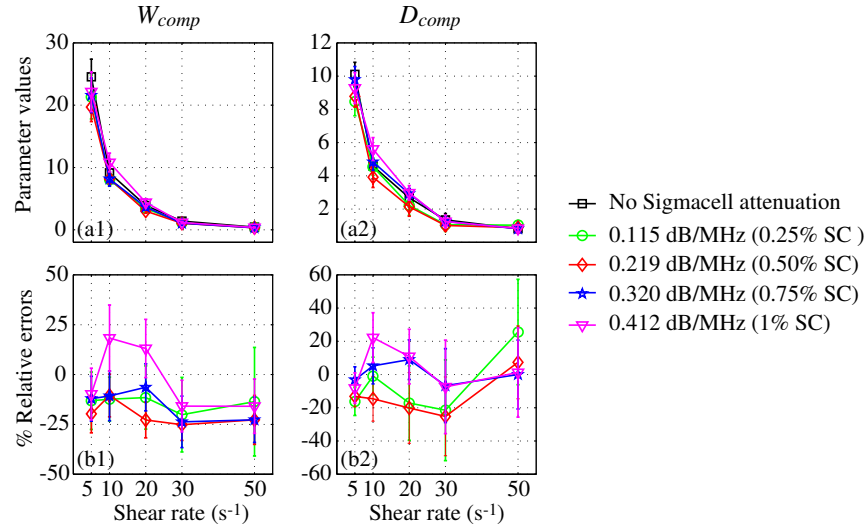


Figure 5: (a) Values of W_{comp} and D_{comp} for the four skin-mimicking phantoms obtained with the SFSE with attenuation-compensation using the attenuation values estimated in reflection. (b) Corresponding relative errors. Parameters W_{comp} and D_{comp} are compared with W_{ref} and D_{ref} .

4.2 Parameters evaluated with the SFSAE

Typical results of the SFSAE minimization procedure for the different agar phantoms at a shear rate of 10 s^{-1} and 50 s^{-1} are given in Fig. 3. For both shear rates, it can be observed that more the total attenuation increases, more the backscattering coefficient amplitude decreases at all frequencies and more the frequency dependence of the backscattering coefficient changes. One can also notice that the parameters W and D from the SFSAE are very similar to the reference parameters W_{ref} and D_{ref} , as well as the total attenuation α_0 from the SFSAE similar to the reference total attenuation. The reference total attenuation α_{ref} corresponds to $\alpha_{sc}e_{sc} + \alpha_{blood}e_{blood}$ where α_{sc} and α_{blood} are the skin-mimicking phantom attenuation and the blood attenuation estimated in the reflection mode as shown in section 3.3.

For each residual shear rate, parameters W , D and α_0 were estimated by the SFSAE. Figure 4 summarizes these results. In this figure, the relative errors for each parameter correspond to: $(W - W_{ref})/W_{ref}$, $(D - D_{ref})/D_{ref}$ and $(\alpha_0 - \alpha_{ref})/\alpha_{ref}$. Except for the shear rate 5 s^{-1} with the skin-mimicking phantom having the smallest attenuation (0.25% SC), the SFSAE gave quantitatively satisfactory estimates of W and D with relative errors below 25%.

4.3 Parameters evaluated with the SFSE with compensation for blood attenuation

The packing factor W_{comp} and the diameter of the aggregates D_{comp} were also evaluated by compensating the backscatter coefficients in the SFSE with the value measured in reflection. Results are presented in Fig. 5. The relative errors are below 25% for all shear rates and all skin-mimicking phantoms.

5. Conclusions

The accuracy of the estimates obtained with the SFSAE was as satisfactory as those obtained with the SFSE with attenuation-compensation (i.e when a priori are known about the attenuation). For both methods, relative errors for W and D were below 25%, except for one value corresponding at the shear rate 5 s^{-1} with the skin-mimicking phantom having the smallest attenuation (0.25% SC). In this last case, the SFSAE gave less accurate estimates (relative errors around 50% for W and α_0). The SFSAE seems to reach its limit of applicability for large aggregate sizes: typically $D_{ref} = 10.11$ (i.e. $kR=2.8$)

Nevertheless, the SFSAE has the major advantage to be easily applicable in vivo because of the simultaneous estimation of the blood structural properties and total attenuation (contrary to the SFSE attenuation-compensation method, needing the attenuation and thickness of the tissue intervening layers to be known).

Acknowledgments

This work was supported by the Canadian Institutes of Health Research (grants #MOP-84358 and CMI-72323), by the Heart and Stroke Foundation of Canada (grant #PG-05-0313), and by the National Institutes of Health of USA (grant #RO1HL078655). Dr Cloutier is recipient of a National Scientist award of the Fonds de la Recherche en Santé du Québec. We are also thankful to Dr F. Destrempe for his helpful discussion on the optimization tool.

References and links

- ¹F. T. H. Yu and G. Cloutier, “Experimental ultrasound characterization of red blood cell aggregation using the structure factor size estimator”, *J. Acoust. Soc. Am.* **122**, 645-656 (2007).
- ²V. Roberjot, S. L. Bridal, P. Laugier, and G. Berger, “Absolute backscatter coefficient over a wide range of frequencies in a tissue-mimicking phantom containing two populations of scatterers”, *IEEE Trans. Ultras., Ferroelect., Freq. Contr.* **43**, 970-978 (1996).
- ³T. A. Bigelow, M. L. Oelze, and W. D. O’Brien, “Estimation of total attenuation and scatterer size from backscatter ultrasound waveforms”, *J. Acoust. Soc. Am.* **117**, 1431-1439 (2005).
- ⁴P. He and J. F. Greenleaf, “Application of stochastic analysis to ultrasonic echoes - Estimation of attenuation and tissue heterogeneity from peaks of echo envelope”, *J. Acoust. Soc. Am.* **79**, 526-534 (1986).
- ⁵B. J. Oosterveld, J. M. Thijssen, P. C. Hartman, R. L. Romijn, and G. J. E. Rosenbusch, “Ultrasound attenuation and texture analysis of diffuse liver disease: methods and preliminary results”, *Phys. Med. Biol.* **36**, 1039-1064 (1991).
- ⁶E. Franceschini, Y. T. H. Yu, and G. Cloutier, “Simultaneous estimation of attenuation and structure parameters of aggregated red blood cells from backscatter measurements”, *J. Acoust. Soc. Am.* **123**, EL85-91 (2008).
- ⁷L. Y. L. Mo and R. S. C. Cobbold, “Theoretical models of ultrasonic scattering in blood”, in *Ultrasonic Scattering in Biological Tissues*, edited by K. K. Shung and G. A. Thieme (CRC, Boca Raton, FL, 1993), Chap. 5, pp. 125-170.
- ⁸V. Twersky, “Low-frequency scattering by correlated distributions of randomly oriented particles”, *J. Acoust. Soc. Am.* **81**, 1609-1618 (1987).
- ⁹K. K. Shung, “On the ultrasound scattering from blood as a function of hematocrit”, *IEEE Trans. Ultras., Ferroelect., Freq. Contr.* **SU-26**, 327-331 (1982).
- ¹⁰S. H. Wang and K. K. Shung, “An approach for measuring ultrasonic backscattering from biological tissues with focused transducers”, *IEEE Trans. Biomed. Eng.* **44**, 549-554 (1997).
- ¹¹B. I. Raju and M. A. Srinivasan, “High-frequency ultrasonic attenuation and backscatter coefficients of *in vivo* normal human dermis and subcutaneous fat”, *Ultrasound in Med. Biol.* **27**, 1543-1556 (2001).